INTERNATIONAL JOURNAL FOR NUMERICAL METHODS IN FLUIDS, VOL. 17, 463–475 (1993)

A MONOTONE STREAMLINE UPWIND METHOD FOR QUADRATIC FINITE ELEMENTS*

D. L. HILL† AND E. A. BASKHARONE‡

Department of Mechanical Engineering, Texas A&M University, College Station, TX 77843-3123, U.S.A.

SUMMARY

A direct streamline upwind method has been developed for convection-dominated flow problems utilizing quadratic elements. The approach presented retains the curve-sidedness feature offered by these elements. This facilitates the use of boundary conforming elements in domains that possess extreme curvature such as turbomachinery bladed components, for which the method is particularly suited. Three test cases are solved to evaluate the stability and diffusive characteristics of the numerical solution. The results presented clearly demonstrate that the proposed method does not exhibit any non-physical spatial oscillations, nor does it suffer from the traditional problem of excessive numerical diffusion.

KEY WORDS Finite elements Streamline upwind Quadratic elements

INTRODUCTION

Numerical solution of the convection dominated flow problem has proved to be a difficult task. Central difference methods and the conventional Galerkin method, being the equivalent finite element counterpart, have consistently yielded unphysical oscillatory solutions.[1–4] Symmetric treatment of the convection terms in these numerical techniques has been identified as the source of the numerical stability problem. This is true in the sense that second-order differencing of the convection terms will naturally produce a set of equations that are decoupled between adjacent nodes when no physical diffusion exists in the flow-governing equations.

Physical reasoning suggests that a non-symmetric or directional treatment of the convective terms would be more appropriate. This is especially true for convection-dominated subsonic flows. Numerical algorithms using this idea have traditionally focused on weighting the convection effects in the direction upstream of the local velocity vector. While this approach helps to stabilize the calculations, it simultaneously introduces unwanted numerical diffusion. The effect of numerical (or cross-stream) diffusion is to smear the solution in areas of high gradients of the flow field. A review of 19 finite difference methods by Smith and Hutton[5] concluded that none of these methods provide a satisfactory performance. Work reported after this review generally demonstrated that further reductions in the amount of numerical diffusion were obtained with the finite difference method.[6,7]

* This study was funded by the Turbomachinery Research Consortium, contract number 32519-15190

† Ph.D. candidate, formerly senior engineer with Pratt & Whitney Aircraft, West Palm Beach, Florida, U.S.A.

‡ Associate Professor

0271-2091/93/180463-13$11.50

Received July 1992
Revised January 1993

Upwinding techniques, originally devised for finite difference algorithms, have been applied with good success to finite element methods. One such approach is known as the streamline upwind Petrov–Galerkin method (SU/PG).[8] This method modifies the weighting functions using the local velocity in such a way as to secure an upstream bias of these functions. This approach was developed using four-noded bi-linear elements and was next applied using linear triangular elements.[9] This technique is currently the most widely used finite element upwind method.[10–12] However, it does exhibit oscillatory behaviour of varied magnitude depending upon the discretization pattern. The SU/PG method has recently been improved by forcing the technique to satisfy the maximum principle,[13] with the discretization unit being the simple linear triangle elements.[14] This work clearly shows that satisfying the maximum principle will ensure the monotonic behaviour of the solution variable.

Another successful streamline upwind method was reported by Rice and Schnipke.[15] Instead of modifying the weighting functions, these authors adopted a direct approach whereby the convection term is evaluated along the local streamline. Calculations presented by Rice and Schnipke showed that this method is monotonic and will introduce tolerable amounts of diffusion into the solution. This work was based on a simple straight-sided four-noded bi-linear finite element and was later extended to three-dimensional applications using conceptually the same element type, namely the eight-noded bi-linear finite element.[16]

The restriction of streamline upwinding to linear elements, as is currently the case, precludes the geometric flexibility and high-order interpolation advantages which quadratic finite elements offer. Initial attempts to apply upwinding techniques to two-dimensional finite element algorithms were made using eight-noded quadratic elements of the so-called 'Serendipity' family and nine-noded Lagrangian elements.[17–19] The approach was based on modifying the weighting functions according to the cell Peclet number and the direction of the average velocity vector. As perhaps should be expected, the numerical results reported showed excessive cross-stream diffusion.

Another method using the nine-noded Lagrangian element was developed by Donea *et al.*[20] Their method employs a generalized governing equation which is obtained by subtracting from the original differential equation the scalar product of its gradient by a vector of free parameters associated with each of the co-ordinate directions. However, the test cases presented in this study revealed solutions which were as oscillatory as those obtained using the Galerkin finite element method.

More recently, an upwind method reported by Tabata and Fujima[21] was developed for quadratic triangular elements. In presenting this method, the authors claimed that the method could approach third-order accuracy. However, examination of this method revealed that this upwinding methodology is not derived on an element-by-element basis. In fact, location of the upstream and downstream upwinding points will span across elements. The results presented did not allow for an objective evaluation of the stability characteristics or numerical diffusion. Although quadratic elements were used, all calculations were performed using straight-sided elements.

This paper presents a streamline upwind method for quadratic elements whereby the advection terms are directly evaluated along a local streamline. The proposed method preserves the geometric flexibility associated with the curve-sidedness of the element by performing the upwinding scheme in the transformed (or local) frame of reference. Test cases will show that the new method yields no fictitious oscillations and that the numerical solutions possess very little numerical diffusion. In addition, the use of quadratic elements in the current method conceptually allows equal-order segregated finite element methods to use higher order interpolation for the pressure within the primitive-variable formulation of the Navier–Stokes equations. Solution of a Poisson-type equation for pressure, in this case, will approach a third-order convergence rate,[22] which is a substantially faster rate in comparison with the same algorithm using a linear element.

ANALYSIS

In this section, we consider the steady two-dimensional advection–diffusion equation

$$\rho u \frac{\partial \phi}{\partial x} + \rho v \frac{\partial \phi}{\partial y} = k\left(\frac{\partial^2 \phi}{\partial x^2} + \frac{\partial^2 \phi}{\partial y^2}\right), \tag{1}$$

where ρ, u, v and k are the given density, velocity components and diffusivity coefficient, respectively, with ϕ being a general field variable. Assuming constant diffusivity, the general form of the finite element formulation for this equation is given by

$$\int_{A^{(e)}} W_i\left(\rho u \frac{\partial \phi}{\partial x} + \rho v \frac{\partial \phi}{\partial y}\right) \mathrm{d}A = k \int_{A^{(e)}} \frac{\partial W_i}{\partial x}\frac{\partial W_j}{\partial x} + \frac{\partial W_i}{\partial y}\frac{\partial W_j}{\partial y} \,\mathrm{d}A\, \phi_j, \tag{2}$$

where $A^{(e)}$ is the element area. The final form of the diffusion term is obtained through integration by parts.[23] Development of the advection term follows in the next section.

Streamline upwind formulation

Details for the streamline upwind method are given for the eight-noded element of the Serendipity family (Figure 1). For pure advection problems, Galerkin's method of weighted residuals yields

$$\int_{A^{(e)}} W_i\left(\rho u \frac{\partial \phi}{\partial x} + \rho v \frac{\partial \phi}{\partial y}\right) \mathrm{d}A = 0, \tag{3}$$

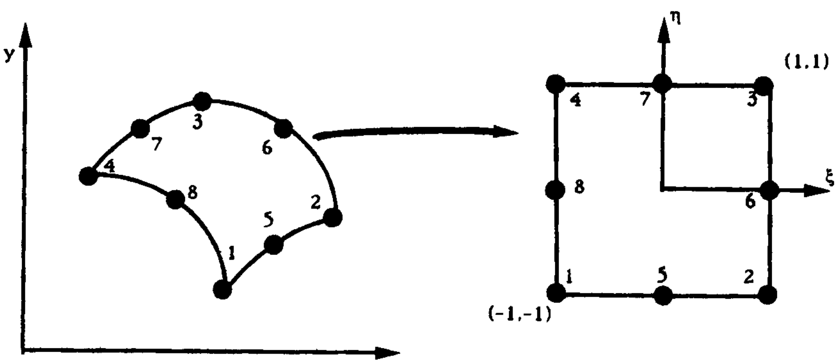

$$\phi(\eta,\xi) = \sum_{i=1}^{8} \phi_i N_i(\eta,\xi)$$

$$x(\eta,\xi) = \sum_{i=1}^{8} x_i N_i(\eta,\xi)$$

$$y(\eta,\xi) = \sum_{i=1}^{8} y_i N_i(\eta,\xi)$$

Figure 1. Eight noded quadratic element from the serendipity family

where W_i are the weighting functions. In streamline co-ordinates, this equation assumes the following form:

$$\int_{A^{(e)}} W_i \rho u_s \frac{\partial \phi}{\partial s} \, dA = 0, \tag{4}$$

where u_s is the velocity in the streamwise direction. On an element level, we can assume that the following relationship[15] is valid:

$$\rho u_s \frac{\partial \phi}{\partial s} = \text{constant}. \tag{5}$$

This will allow equation (4) to be rewritten as

$$\rho u_s \frac{\partial \phi}{\partial s} \int_{A^{(e)}} W_i \, dA = 0. \tag{6}$$

Evaluation of this expression requires definition of an upwind point every time a downwind point is detected. The process for identifying downwind nodes is straightforward. For each node, we need to determine if the negative of the velocity vector points back into the element. This is stated mathematically as

$$\begin{aligned} -v_j\left(\frac{\partial x}{\partial \xi}\partial\xi+\frac{\partial x}{\partial \eta}\partial\eta\right)^+ + u_j\left(\frac{\partial y}{\partial \xi}\partial\xi+\frac{\partial y}{\partial \eta}\partial\eta\right)^+ &\geq 0, \\ -v_j\left(\frac{\partial x}{\partial \xi}\partial\xi+\frac{\partial x}{\partial \eta}\partial\eta\right)^- + u_j\left(\frac{\partial y}{\partial \xi}\partial\xi+\frac{\partial y}{\partial \eta}\partial\eta\right)^- &\geq 0. \end{aligned} \tag{7}$$

The negative and positive superscripts indicate the two different sides of the element that join at the computational node (Figure 2). Both conditions have to be met for corner nodes. For mid-side nodes, only the first condition has to be satisfied.

Once a downwind node is detected the mass flow rates, defined in Figure 3, are calculated using Simpson's rule of integration. It should be emphasized that the quadratic variation of the velocity field is retained in performing the integration. As an example, to obtain the flow rates finxa and finxb (Figure 3), the mass flow rate along side (1–8–4) is first evaluated using quadratic shape functions. Then, side (8–4) is handled similarly giving rise to finxa. The difference between the two values provides finxb. This technique is applied to all element boundaries.

The computed mass flow rates allow the upstream point of the streamline associated with any downwind node to be determined. The methodology used to locate the upstream point has been

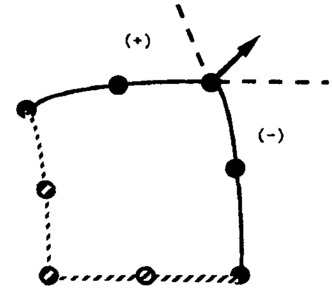

Figure 2. Downwind node detection notation

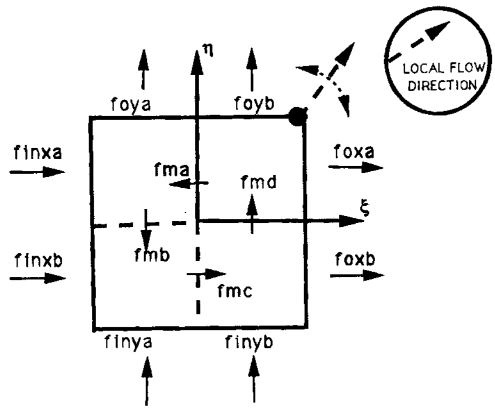

Figure 3. Definition of mass flow rates

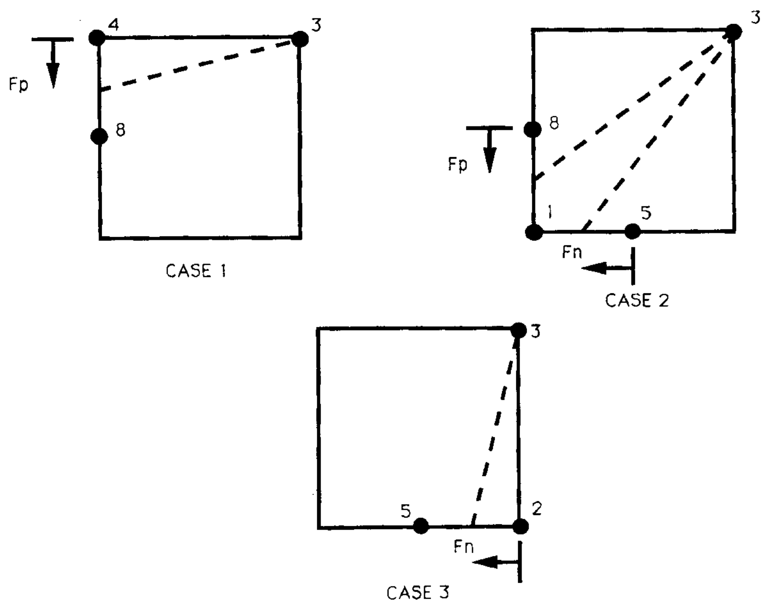

Figure 4. Upwinding stencil logic for corner nodes

developed in a generic stencil format. This allows easy cycling through all nodes. As an example, the orientation of the stencil for node 3 is shown in Figure 4. This figure shows the different possible scenarios that could occur. In a generic format, this logic will be the same for all corner nodes. The pointers shown in Figure 4 are evaluated using the ratios of the mass flow rates defined previously. The location and values of the pointers will ultimately determine all nodal contributions.

A similar approach is applied for mid-side nodes. However, the stencil design for these nodes is slightly different (Figure 5). The choice of which stencil is used is based on the sign of the mass flux

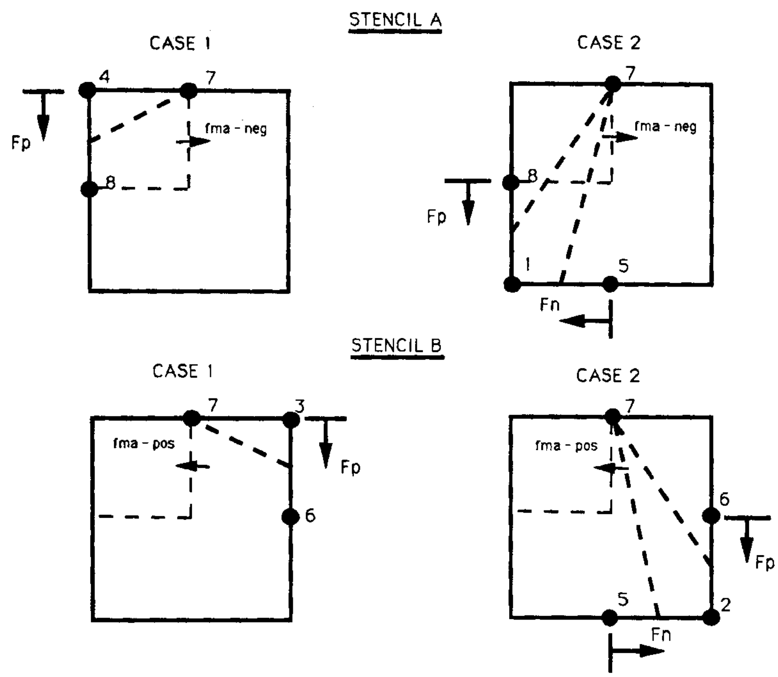

Figure 5. Upwinding stencil logic for mid-side nodes

across the fictitious internal surfaces of the element (Figure 3). For example, the stencil used for node 7 would be determined by the sign of the mass flux, fma. Calculation of these internal fluxes is also obtained by Simpson's rule of integration.

With the upstream point located, the next step is to evaluate equation (6). The product ρu_s is obtained from the values of the current downwind node. For instance, should node 3 be the current downwind point, the value of the streamline velocity would be

$$u_s = \sqrt{[(u_3^2 + v_3^2)]}. \tag{8}$$

The value of $\partial\phi/\partial s$ is generally obtained by tracing the streamline within the finite element. For a bi-linear finite element,[15] this will result in a straight line approximation of the streamline. With a curve-sided element, the curvature effects are naturally included into the calculations by tracing the streamline in the transformed computational domain. The following approximation, which implies sufficiently small element dimensions, is made:

$$\frac{\partial\phi}{\partial s} \approx \frac{\Delta\phi}{\Delta s}, \tag{9}$$

where $\Delta\phi$ is the difference between the upstream and downstream scalar values. Δs is calculated using the following formula:

$$\Delta s = \sqrt{[(\Delta x^2 + \Delta y^2)]}, \tag{10}$$

Table I. Advection contributions for example case

	0·0	0·0	0·0	0·0	0·0	0·0	0·0	0·0
	0·0	0·0	0·0	0·0	0·0	0·0	0·0	0·0
	$-\mathrm{Fp}^*\mathrm{Fn}^*A$	0·0	A	0·0	$(\mathrm{Fn}-1)^*A$	0·0	0·0	$(\mathrm{Fp}-1)^*A$
$A=\int W_3\,\mathrm{d}A$	0·0	0·0	0·0	0·0	0·0	0·0	0·0	0·0
	0·0	0·0	0·0	0·0	0·0	0·0	0·0	0·0
	0·0	0·0	0·0	0·0	0·0	0·0	0·0	0·0
	0·0	0·0	0·0	0·0	0·0	0·0	0·0	0·0
	0·0	0·0	0·0	0·0	0·0	0·0	0·0	0·0

which can be rewritten as

$$\Delta s=\sqrt{\left[\left(\frac{\partial x}{\partial \xi}\mathrm{d}\xi+\frac{\partial x}{\partial \eta}\mathrm{d}\eta\right)^2+\left(\frac{\partial y}{\partial \xi}\mathrm{d}\xi+\frac{\partial y}{\partial \eta}\mathrm{d}\eta\right)^2\right]}. \tag{11}$$

The final step is to assemble the elemental contributions. For illustration purposes the reader is referred to the example in Figure 4, where node 3 is the only downwind node with the upstream point falling between nodes 8 and 1. Table I shows the advection stiffness matrix that would result. Fp and Fn would be obtained (by reference to Figures 3 and 4) from the ratios of the mass fluxes.

$$\mathrm{Fp}=\max\{\min\{(\mathrm{foya}+\mathrm{foyb})/(\mathrm{finxa}+\mathrm{finxb}),1\},0{\cdot}0\}$$
$$\mathrm{Fn}=\max\{\min\{(\mathrm{foxa}+\mathrm{foxb})/(\mathrm{finya}+\mathrm{finyb}),1\},0{\cdot}0\} \tag{12}$$

For this example, Fn = 1 and Fp would fall between 0·0 and 1·0.

RESULTS

The merit of the new upwinding technique will be appraised in this section through three test cases. The first case is the skewed flow field advection problem depicted in Figure 6. This type of

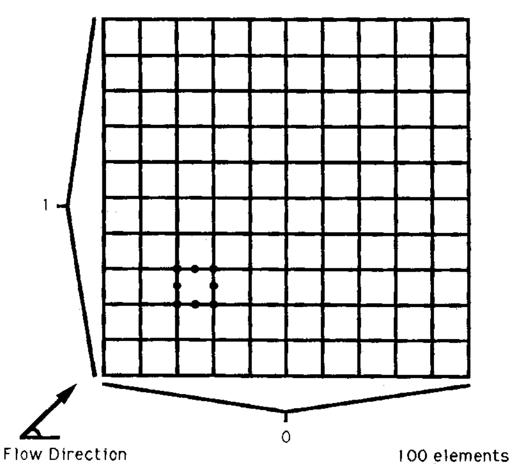

Figure 6. Problem and model description for test case No. 1

problem is considered to be a worst case scenario for any upwinding method. With the diffusivity set equal to 0·0, the cell Peclet number (uL/k) approaches infinity. Typical results obtained using the Galerkin formulation for a uniform flow at 45° are shown in Figure 7. The numerical oscillations shown in this figure are more or less representative of the outcome of any method that equally weights the advection terms in the upstream and downstream flow directions. Poor performance make such methods hardly applicable to problems involving steep gradients of the convected field variable(s).

A solution based on the Rice and Schnipke approach[15] and using a bi-linear finite element is shown in Figure 8 for a uniform flow of 64°. The diffusion effects were virtually eliminated by setting the diffusivity coefficient equal to 10^{-6}. As seen in the figure, the solution predicted is smooth and monotonic. For the bi-linear element, the maximum error was reportedly encountered for flow angles of 64 and 27°,[15] while exact nodal answers were obtained for flow angles of 0, 45 and 90°.

The new upwinding scheme was tested for flow angles of 27, 45 and 64°. The results from these calculations are shown in Figures 9(a)–9(c). As seen in these figures, exact nodal results were obtained for each flow angle. For this test case, the maximum amount of numerical diffusion

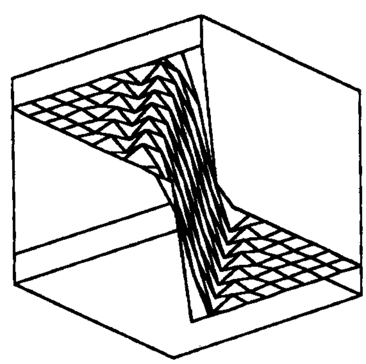

Figure 7. 45° flow case using the Galerkin weighted residual method

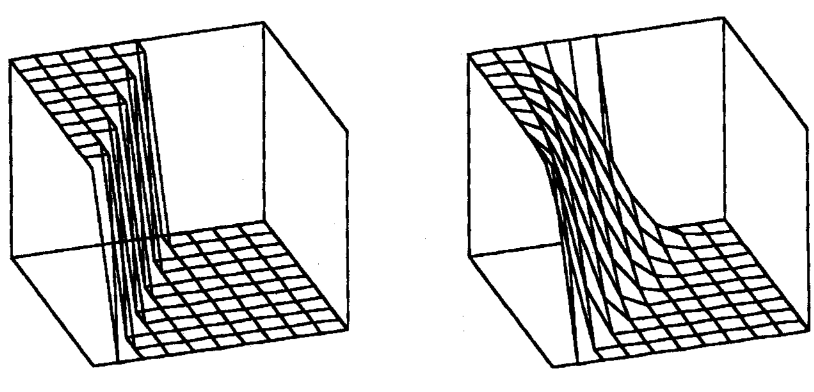

Figure 8. 64° skewed advection case using the bi-linear element

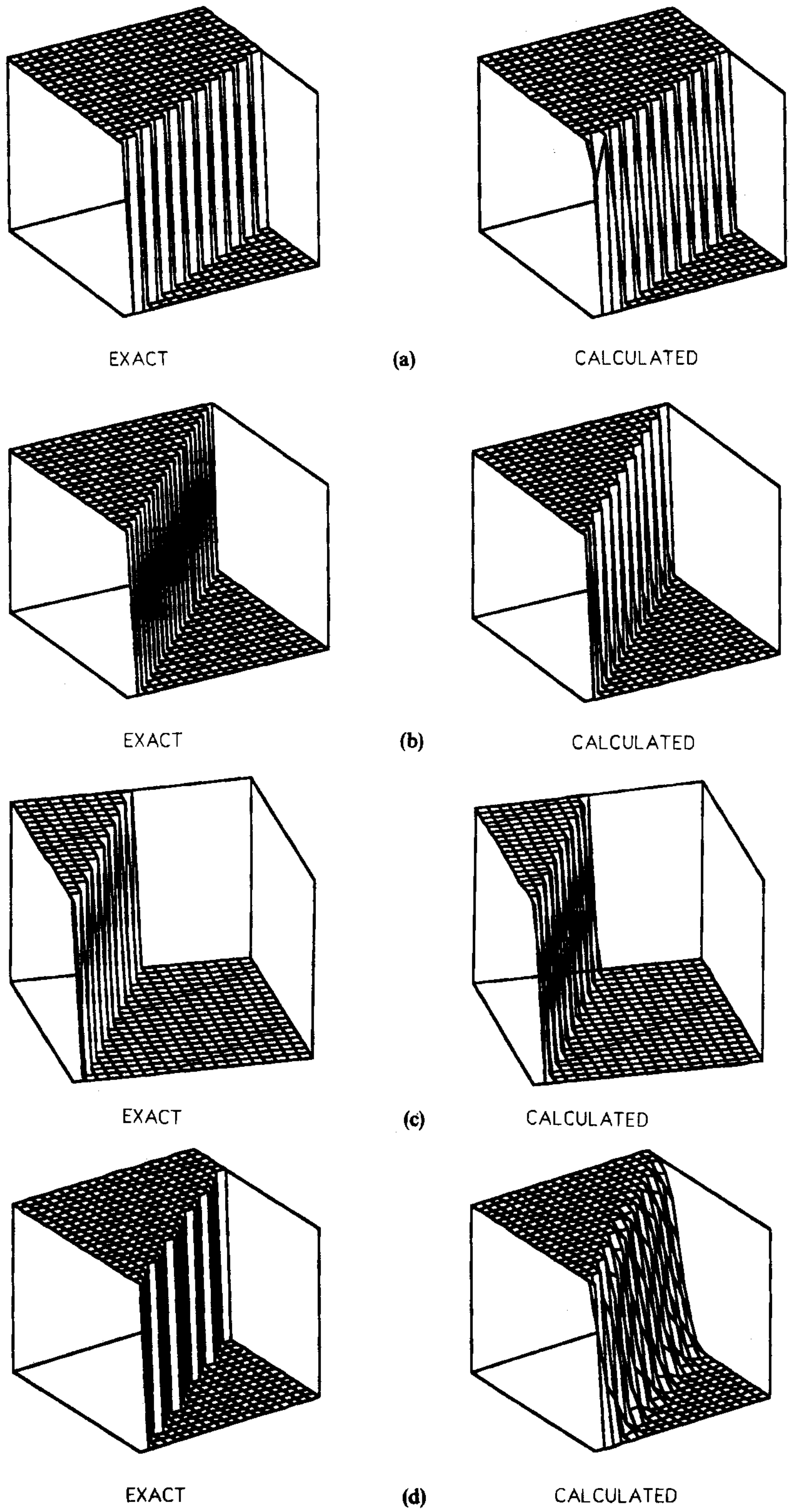

Figure 9. Skewed advection for (a) 27° flow, (b) 45° flow, (c) 64° flow and (d) 36·8° flow

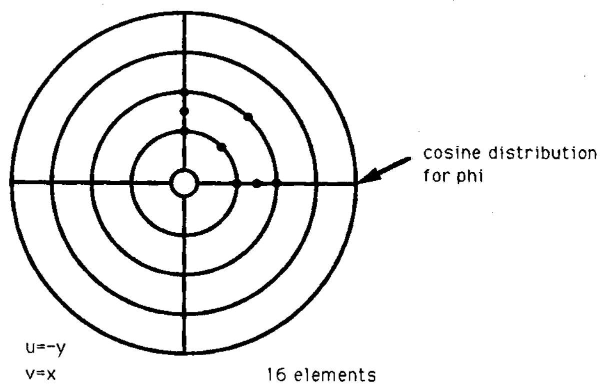

Figure 10. Problem description for test case No. 2

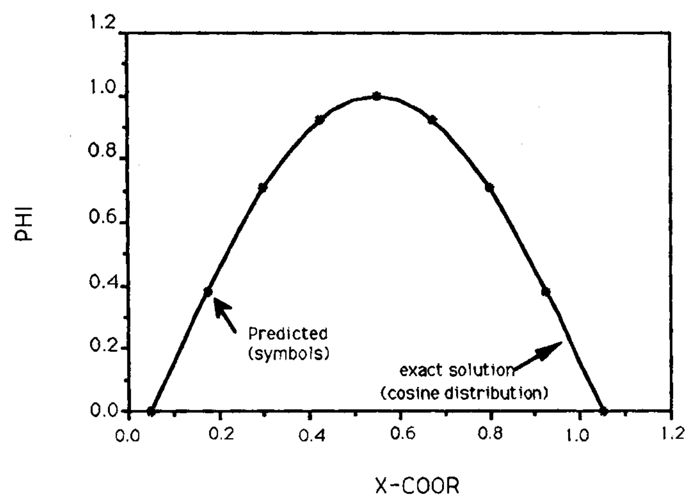

Figure 11. Comparison between inlet and exit profiles

prevails at flow angles of approximately 14, 36·8, 53·1 and 75·9°. The 36·8° flow-angle case is shown in Figure 9(d). These calculations illustrate the improvement in accuracy that is obtained when the quadratic element is used as the discretization unit.

The second test case demonstrates the advantage of the curve-sidedness capability of the quadratic element. This problem was derived from the Smith and Hutton test case[5] and is described in Figure 10. The object of this test case is to assess the advection of a 'cosine profile' in a complete circle. The u-velocity is set equal to $-y$ and the v-velocity is set to x. Note that any smearing of the profile in this case would be indicative of fictitious dissipation. However, examination of the results shown in Figure 11 indicate no smearing of the initial profile. Furthermore, the reader is reminded that the geometry of the domain would have been significantly distorted had a comparable number of bi-linear elements been used instead.

The third test case concerns the advection–diffusion of a temperature field in a rotating hollow shaft.[24] Because of the domain symmetry, the problem can be reduced to a one-dimensional

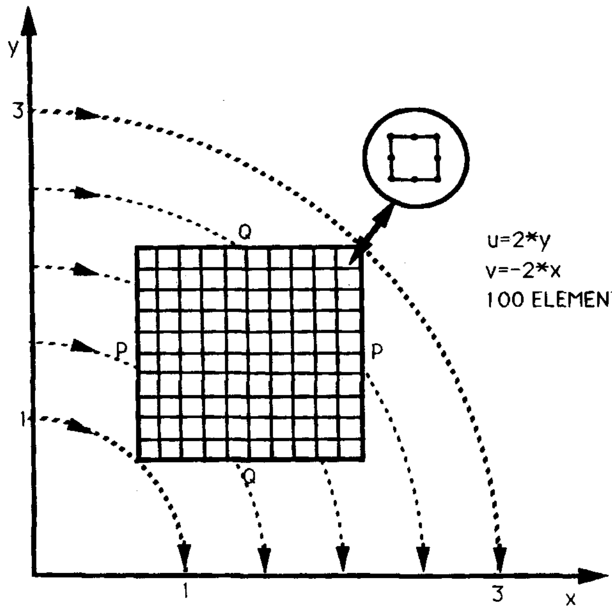

Figure 12. Problem and model description for test case No. 3

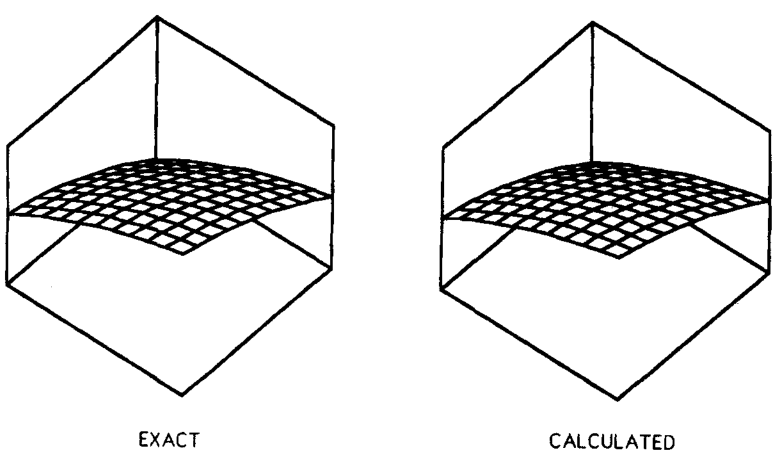

Figure 13. Calculated solution is smooth and monotonic

equation governing the transport of temperature in the radial direction. However, selection of Cartesian co-ordinates forces the problem to be of the two-dimensional type. A complete description of the flow physics and finite element model is shown in Figure 12. The conduction coefficient is not constant and is assumed to be proportional to $(x^2+y^2)^{-1}$. Boundary conditions for temperature were taken from the exact solution and imposed on all boundaries of the domain. The calculated solution is compared with the exact solution in Figure 13. The surface plots

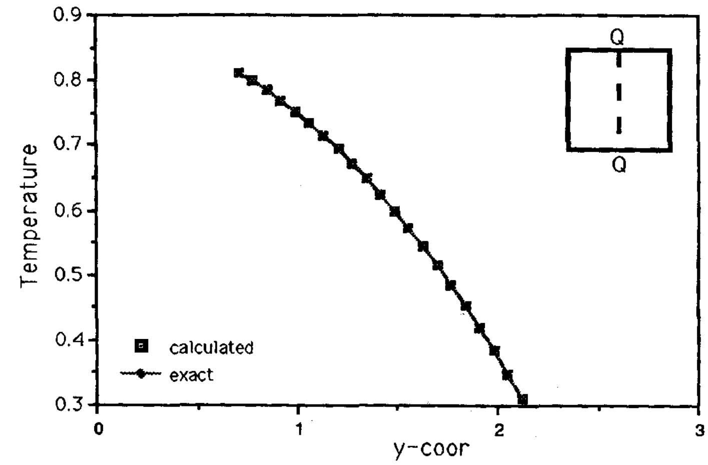

Figure 14. Direct comparison with exact solution for constant X location

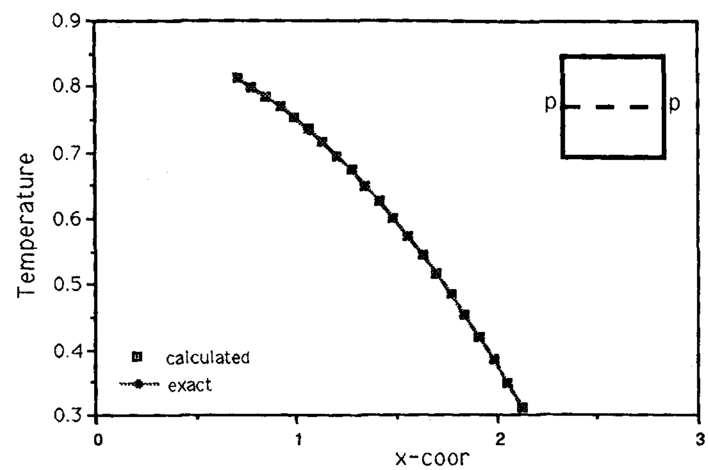

Figure 15. Direct comparison with exact solution for constant Y location

demonstrate the monotonic behaviour of the numerical solution. The accuracy of the calculation can be judged by comparing line plots of the non-dimensional temperature at constant values of x and y as shown in Figures 14 and 15. Examination of these figures reveal an excellent agreement with the exact solution along the P–P and Q–Q locations.

CONCLUSIONS

A new direct streamline upwind method has been developed for quadratic elements. The curve-sidedness of these elements is preserved by performing the upwind procedure in the transformed space. The proposed method has been shown to be accurate for a cell Peclet number of infinity for both straight and curve-sided element models. Excellent agreement was also obtained for a test problem where the convective and diffusive transport processes were of equal importance. Utilization of the new upwinding method in solving convection-dominated flow fields in turbomachinery primary-flow passages is currently in progress.

ACKNOWLEDGEMENT

This study was funded by the Turbomachinery Research Consortium, Texas A&M University.

REFERENCES

1. G. D. Raithby, 'Skew upwind differencing schemes for problems involving fluid flow', *Comput. Methods Appl. Mech. Eng.*, **9**, 153–164 (1976).
2. B. P. Leonard, 'A stable and accurate convective modeling procedure based on quadratic upstream interpolation', *Comput. Methods Appl. Mech. Eng.*, **19**, 59–98 (1979).
3. S. V. Patankar, *Numerical Heat Transfer And Fluid Flow*, Hemisphere, Washington, DC, 1980.
4. P. M. Gresho and R. L. Lee, 'Don't suppress the wiggles, they're telling you something!, finite element methods for convection flow', *ASME AMD*, **34**, 1979.
5. R. M. Smith and A. G. Hutton, 'The numerical treatment of advection: a performance comparison of current methods', *Numer. Heat Transfer*, **5**, 439–409 (1982).
6. K. C. Karki, S. V. Patankar, A. K. Runchal and H. C. Mongla, 'Improved numerical methods for turbulent viscous recirculating flows', *NASA CR-182169*, 1988.
7. B. P. Leonard, 'SHARP simulation of discontinuities in highly convective steady flow', *NASA Technical Memorandum, ICOMP-87-9*, 1987.
8. A. N. Brooks and T. J. R. Hughes, 'Streamline upwind/Petrov–Galerkin for convection dominated flows with particular emphasis on the incompressible Navier–Stokes equations', *Comput. Methods Appl. Mech. Eng.*, **32**, 199–259 (1982).
9. A. Mizukami, 'An implementation of the streamline-upwind/Petrov–Galerkin method for linear triangular elements', *Comput. Methods Appl. Mech. Eng.*, **49**, 357–364 (1985).
10. M. F. Cohen, 'Application of the Petrov–Galerkin method to chemical-flooding reservoir simulation in one dimension', *Comput. Methods Appl. Mech. Eng.*, **41**, 195–218 (1983).
11. T. J. R. Hughes, L. P. Franca, I. Harari, M. Mallet, F. Shakib and T. E. Spelce, 'Finite element method for high-speed flows: consistent calculation of boundary flux', *AIAA 87-02636*, 1987.
12. Q. Zhong and M. D. Olson, 'Finite-element–algebraic closure analysis of turbulent separated–reattaching flow around a rectangular body', *Comut. Methods appl. Mech. Eng.*, **85**, 131–150 (1991).
13. T. Ikeda, *Maximum Principle In Finite Element Models For Convection–Diffusion Phenomena*, North-Holland, 1983.
14. A. Mizukami and T. J. R. Hughes, 'A Petrov–Galerkin finite method for convection-dominated flows: an accurate upwinding technique for satisfying the maximum principle', *Comput. Methods Appl. Mech. Eng.*, **50**, 181–193 (1985).
15. J. G. Rice and R. J. Schnipke, 'A monotone streamline upwind finite element method for convection-dominated flows', *Comput. Methods. Appl. Mech. Eng.*, **47**, 313–327 (1984).
16. Flotran distributed by Compuflo Inc, Charlottesville, VA 22905, U.S.A.
17. I. Christie, D. F. Griffiths, A. R. Mithcell and O. C. Zienkiewicz, 'Finite element methods for second order differential equations with significant first derivatives', *Int. j. numer. methods eng.*, **10**, 1389–1396 (1976).
18. J. C. Heinrich, P. S. Huyakorn and O. C. Zienkiewicz, 'An "upwind" finite element scheme for two-dimensional convective transport equations', *Int. j. numer. methods eng.*, **11**, 131–143 (1977).
19. J. C. Heinrich and O. C. Zienkiewicz, 'Quadratic finite element schemes for two-dimensional convective – transport problems', *Int. j. numer. methods eng.*, **11**, 1831–1844 (1977).
20. J. Donea, T. Belytschko and P. Smolinski, 'A generalized Galerkin method for steady convective – diffusion problems with application to quadratic shape function elements', *Comput. Methods Appl. Mech. Eng.*, **48**, 25–43 (1985).
21. M. Tabata and S. Fujima, 'An upwind finite element scheme for high-Reynolds number flows', *Int. j. numer. methods fluids*, **12**, 305–322 (1991).
22. C. A. J. Fletcher, *Computational Techniques For Fluids Dynamics*, Vol. 1, Chapter 5, Springer, Berlin, 1991.
23. K. H. Huebner and E. A. Thornton, *The Finite Element Method For Engineers*, Wiley, New York, 1982.
24. A. K. Runchal, 'Convergence and accuracy of three finite difference schemes for a two-dimensional conduction and convection problem', *Int. j. numer. methods eng.*, **4**, 541–550 (1972).